ADVANCES IN ATMOSPHERIC SCIENCES, VOL. 36, MARCH 2019, 253–260

• **Original Paper** •

Predictability of South China Sea Summer Monsoon Onset

Gill M. MARTIN*[1], Amulya CHEVUTURI[2], Ruth E. COMER[1], Nick J. DUNSTONE[1], Adam A. SCAIFE[1,3], and Daquan ZHANG[4]

[1]*Met Office Hadley Centre, Met Office, FitzRoy Road, Exeter, EX*1 3*PB, UK*

[2]*NCAS-Climate and Department of Meteorology, University of Reading, Reading, RG*6 6*BB, UK*

[3]*College of Engineering, Mathematics and Physical Sciences, Exeter University, Exeter, EX*4 4*QJ, UK*

[4]*Laboratory for Climate Studies, National Climate Center, China Meteorological Administration, Beijing* 100081*, China*

(Received 1 May 2018; revised 4 September 2018; accepted 11 October 2018)

ABSTRACT

Predicting monsoon onset is crucial for agriculture and socioeconomic planning in countries where millions rely on the timely arrival of monsoon rains for their livelihoods. In this study we demonstrate useful skill in predicting year-to-year variations in South China Sea summer monsoon onset at up to a three-month lead time using the GloSea5 seasonal forecasting system. The main source of predictability comes from skillful prediction of Pacific sea surface temperatures associated with El Niño and La Niña. The South China Sea summer monsoon onset is a known indicator of the broadscale seasonal transition that represents the first stage of the onset of the Asian summer monsoon as a whole. Subsequent development of rainfall across East Asia is influenced by subseasonal variability and synoptic events that reduce predictability, but interannual variability in the broadscale monsoon onset for East Asian summer monsoon still provides potentially useful information for users about possible delays or early occurrence of the onset of rainfall over East Asia.

Key words: SCSSM, South China Sea summer monsoon, EASM, East Asian summer monsoon

Citation: Martin, G. M., A. Chevuturi, R. E. Comer, N. J. Dunstone, A. A. Scaife, and D. Q. Zhang, 2019: Predictability of South China Sea summer monsoon onset. *Adv. Atmos. Sci.*, **36**(3), 253–260, https://doi.org/10.1007/s00376-018-8100-z.

1. Introduction

The broadscale East Asian summer monsoon (EASM) onset occurs in two stages (Wang et al., 2004, 2009). The first stage is a seasonal transition that occurs over the South China Sea (SCS) and is characterized by an abrupt but sustained reversal of the lower-tropospheric zonal winds from easterlies to westerlies. Several studies have considered the SCS summer monsoon (SCSSM) onset as the precursor for EASM development (Tao and Chen, 1987; Lau and Yang, 1997), with the formation and progression of the mei-yu rainband forming the second salient phase (Wang et al., 2004). Predicting monsoon onset is crucial for agriculture and socioeconomic planning in countries where millions rely on the timely arrival of monsoon rains for their livelihoods.

Interannual variability in the seasonal transition that constitutes the broadscale monsoon onset has been shown to be related to thermal conditions over the Tibetan Plateau (Wu et al., 2012), El Niño–Southern Oscillation (ENSO) effects (Zhou and Chan, 2007; Hu et al., 2014; Xie, 2016; Zhu and Li, 2017), regional air–sea interactions (He and Wu, 2013) and intraseasonal oscillations (ISOs; Wu, 2010; Li et al., 2013; Zhu and He, 2013; Shao et al., 2015; Wang et al., 2018). He et al. (2017) carried out a comprehensive analysis of the SCSSM onset in individual years between 1997 and 2014 and showed that the years can be divided into "normal", "intermittent" and "delayed" onset years based on the development of local circulations, thermodynamic conditions and rainfall patterns following the seasonal transition. He et al. (2017) found that eight out of the 18 years they analyzed exhibited intermittent rainfall onset (such that the seasonal dynamical transition is not closely followed by the establishment of monsoon rains and maximum SCS surface temperatures, with a delay caused by an active ISO or northern cold air entering the SCS), and suggested that this reduces the potential predictability of local rainfall onset even if the seasonal dynamical transition may be predictable. Wang et al. (2018) described the effects of the tropical ISO on early, normal and late SCSSM onsets observed over 34 years. They confirmed work from previous studies showing that, before each onset, the SCS is controlled by the dry phase of the ISO (Shao et al., 2015), and the SCS is warmed to precondition the onset; while after each onset, the SCS is cooled by the wet phase of the ISO (Wu, 2010). However, Wang et al. (2018) showed that the transition process is found to be

* Corresponding author: Gill M. MARTIN
Email: gill.martin@metoffice.gov.uk

related to different ISO evolutions over the Indian Ocean for the three types of onsets.

Even in non-intermittent onset years, the progression of rainfall onset over East Asia is rarely smooth. After an initial burst of rainfall over the SCS, the rain band rapidly advances northward before stagnating over the Yangtze and Huai River valleys in the mei-yu front (baiu in Japan). The mei-yu rainband exhibits large intraseasonal and interannual variability and has been the subject of extensive literature [see Ding and Chan (2005) for a review]. Its onset is associated with a northward shift of the Northwest Pacific subtropical high axis to about 25°N and the migration of the upper-level westerly jet over Eurasia to the north of the Tibetan Plateau (Sampe and Xie, 2010; Luo et al., 2013). Li et al. (2018) showed that the anticyclone in the upper troposphere over South Asia in April has a significant relationship with mei-yu onset dates, such that a stronger South Asian anticyclone in April is followed by earlier onset dates of the mei-yu. Despite the complexity associated with these multiple drivers, interannual variability in the seasonal transition that constitutes the broadscale monsoon onset for the Asian summer monsoon as a whole still provides useful information for forecasters about possible delays or early occurrence of the onset of rainfall over East Asia. One of the most-used indices for determining SCSSM onset is that proposed by Wang et al. (2004). This index identifies the first pentad after 25 April in which the zonal wind at 850 hPa over the southern part of the SCS (5°–15°N, 110°–120°E) shifts from a mean easterly to a mean westerly. Wang et al. (2004) demonstrated that this index is highly indicative of the seasonal transition of the large-scale circulation. They showed that the onset variations determined using this index matched the broadscale onset determined by the principal component of the first empirical orthogonal function (EOF) of the low-level winds over East Asia and the western North Pacific. They argued that this simple index avoids the additional complications of the intraseasonal variability that is included in EOF analysis.

An alternative definition for SCSSM onset was proposed by Gao et al. (2001), and is used in operational extended-range forecasting by the China Meteorological Administration (CMA; D. Zhang, personal communication). This includes an additional criterion of a sustained increase of equivalent potential temperature at 850 hPa above 340 K over the SCS region (10°–20°N, 110°–120°E) concurrent with the establishment of westerly winds over the same region. The increase in equivalent potential temperature is considered to indicate sea surface warming, monsoonal transport of moisture into the region and the potential for increased convective activity (Gao et al., 2001; Li et al., 2013; Luo et al., 2013). The region specified by Gao et al. (2001) is further north than that for the Wang et al. (2004) index and includes the northern SCS.

In this paper, we investigate the prediction skill of the SCSSM onset on seasonal time scales in the operational hindcast set of the GloSea5-GC2 seasonal forecasting system. Section 2 outlines the data and methods used in our study; section 3 shows the analysis of predictability of the two onset indicators, including tests of the robustness of the seasonal forecast skill. Discussion and conclusions on the usefulness of the seasonal forecast skill of the broadscale monsoon onset using these SCSSM onset indicators are included in section 4.

2. Data and methods

Daily and pentad time series of 850-hPa zonal winds (U_{850}), air temperature (T_{850}) and specific humidity (q_{850}) from the 23-year set of hindcasts (1993–2015) made with the GloSea5-GC2 operational long-range forecast system (MacLachlan et al., 2015; Williams et al., 2015) are taken from four start dates (17 and 25 March; 1 and 9 April). This represents a greater than one-month lead time for the average SCSSM onset date of mid May. The standard operational hindcast set includes seven members per start date. To investigate the robustness of our results, and the dependence on ensemble size, we make use of an additional hindcast ensemble, using the same model configuration and also with seven members per start date (except for 17 March, for which there are only three members). Further, to investigate changes with lead time, we repeat the analysis for a 56-member ensemble of start dates on 25 March, and 1, 9 and 17 April, and for 28-member ensembles generated using the four start dates (1, 9, 17 and 25) of January, February and March respectively.

Data representative of observations are taken from ERA-Interim (Dee et al., 2011) for the same years. Equivalent potential temperature is calculated from the temperature and humidity fields at 850 hPa using the formula in Bolton (1980). Sea surface temperatures (SSTs) for March (used in section 3.3) are taken from the HadISST1.1 dataset (Rayner et al., 2003).

SCSSM onset is determined using the criteria established by Wang et al. (2004) and Gao et al. (2001). According to Wang et al. (2004), the onset date is the first pentad after 25 April (i.e., pentad 24 onwards) when the area-averaged U_{850} over the southern SCS (5°–15°N, 110°–120°E, denoted U_{SCS}) is (i) greater than 0 m s^{-1}; (ii) in the subsequent four pentads (including the onset pentad), U_{SCS} must be positive in at least three pentads; and (iii) the accumulated four-pentad mean U_{SCS} is greater than 1 m s^{-1}. Wang et al. (2004), He and Zhu (2015) and Zhu and Li (2017) compared the SCSSM onset pentads between different reanalyses, including NCEP-1 and −2 [Kalnay et al. (1996) and Kanamitsu et al. (2002) respectively], as well as ERA-Interim, and showed reasonable correlations between them (generally > 0.8).

Gao et al. (2001) suggested an onset criterion based on the area-averaged 850-hPa pentad equivalent potential temperature (θ_e) and U_{850} over the region (10°–20°N, 110°–120°E), with the onset date being the first pentad when θ_e is greater than 340 K[a] and U_{850} is greater than 0.0 m s^{-1}, stably (i.e., persists for at least three pentads followed by a break of no more than two pentads, or for two pentads followed by a

[a]Originally specified as 335 K by Gao et al. (2001) but revised to 340 K by Ding and He (2006).

break of no more than one pentad). It should be noted that the region of consideration for this index is slightly further north than that considered by Wang et al. (2004).

3. Results

3.1. *Prediction skill of SCSSM onset using the Wang et al. (2004) criterion*

Figure 1 shows the SCSSM onset pentads identified using the Wang et al. (2004) criterion for each forecast member with start dates of 17 and 25 March, and 1 and 9 April, in each year, with the ensemble-mean pentad and that identified in the reanalyses. The average interannual standard deviation of onset dates from individual ensemble members is 2.2 pentads, which compares reasonably well with that of the reanalyses (2.6 pentads), and there is a statistically significant (at the 0.75% level, for a one-tailed t-test) correlation of 0.5 between the interannual variations of the ensemble-mean dates and those from the reanalyses, indicating significant predictability. The hindcasts also predict the mean onset pentad to match that of the reanalyses, i.e., pentad 28 (16–20 May).

Luo and Lin (2017) suggested that a more objective measure of the SCSSM onset can be determined using a daily cumulative U_{SCS} and specifying the onset as where this time series changes from decreasing to increasing (indicating that the flow is becoming predominantly westerly). Wang et al. (2004) also checked their SCSSM onset dates against a cumulative U_{SCS} criterion, DU, which compares the accumulated U_{SCS} in the three days prior to and after the onset. They showed that, although their onset criteria do not explicitly require an abrupt change in westerly speed across the onset pentad, the resultant onset pentads were coincident with such a change. We found that including the additional criterion of DU > 7 m s^{-1} makes very little difference to our results (not shown).

We carried out the same analysis for four start dates (1, 9, 17 and 25) in January, February and March taken from the standard operational hindcast ensemble of seven members per start date, and also for a 56-member combined ensemble using start dates of 25 March, and 1, 9 and 17 April (see Table 1). The correlation coefficient increases with decreasing lead time, becoming statistically significant at the 1.5% level (for a one-tailed t-test) from February start dates onwards. Thus, there is significant skill in the SCSSM onset prediction using the Wang et al. (2004) index at a near three-month lead time over this hindcast period.

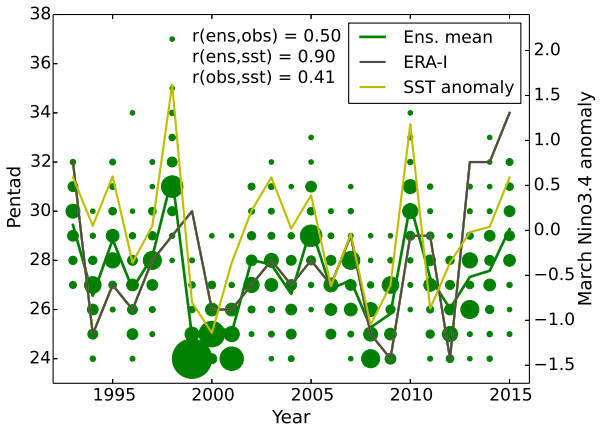

Fig. 1. Predictability of the SCSSM wind onset: onset pentads derived using the method proposed by Wang et al. (2004) from the GloSea5 ensemble predictions initialized on 17 and 25 March, and 1 and 9 April (green dots represent individual members of the 52-member ensemble, with the size of the dot scaled by the number of members predicting the same onset pentad), and their ensemble mean (green line), compared with the equivalent onset pentads derived from ERA-Interim (black line). The yellow line shows the Niño3.4 SST anomaly in March for each year taken from the HadISST1.1 dataset. Pearson correlation coefficients are given in the legend: r (ens, obs) represents the correlation between the GloSea5 ensemble mean and ERA-Interim; r (ens, sst) represents the correlation between the GloSea5 ensemble mean SCS onset pentads and the observed March Niño3.4 SST anomaly; r (obs, sst) represents the correlation between the ERA-Interim SCS onset pentads and the observed March Niño3.4 SST anomaly.

3.2. *Predictability of SCSSM onset using the Gao et al. (2001) criterion*

Figure 2 shows the SCSSM dates identified using the Gao et al. (2001) criterion in each year by each of the 52 ensemble members with start dates of 17 and 25 March, and 1 and 9 April, with the ensemble-mean pentad and that identified in the reanalyses. In contrast with the findings using the Wang et al. (2004) U_{SCS} index, we find low skill in onset prediction using the Gao et al. (2001) index at a greater than one-month lead time. Table 1 shows that the correlation increases

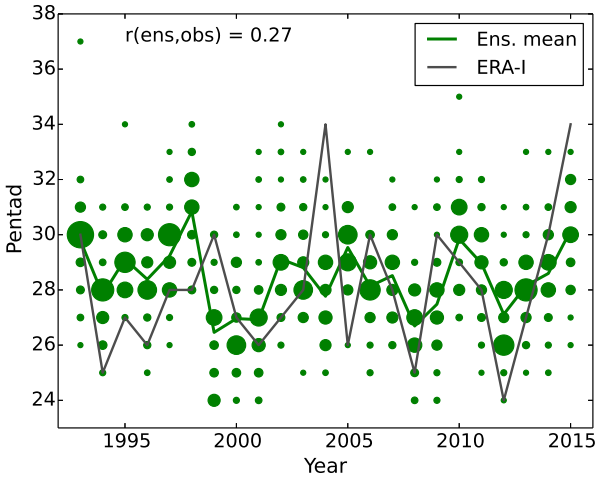

Fig. 2. As in Fig. 1 but for SCSSM thermodynamic onset as determined by a sustained increased of θ_e above 340 K accompanied by the establishment of westerly winds over the region (10°–20°N, 110°–120°E), as proposed by Gao et al. (2001) [with the threshold modified by Ding and He (2006)].

Table 1. Pearson correlation coefficients between ensemble-mean SCSSM onset dates from GloSea5 and those from ERA-Interim, using the definitions of Wang et al. (2004) and Gao et al. (2001), for different hindcast start dates. Note that the earliest observed SCSSM onset date is pentad 25 (1–5 May), and the mean onset date is pentad 28 (16–20 May). Where just the month is shown, start dates are 1, 9, 17 and 25 of the month. Correlation coefficients statistically significant (for a 23-year hindcast period) at the less than 1.5% level for a one-tailed test are set in italics, and those significant at the less than 1% level for a one-tailed test are set in bold.

	Ensemble start dates				
	January	February	March	17 and 25 March; 1 and 9 April	25 March; 1, 9 and 17 April
Wang et al. (2004)	0.28	*0.46*	*0.45*	**0.50**	**0.53**
Gao et al. (2001)	-	-	-	0.27	0.30

slightly if the lead time is reduced to around one month, but remains barely statistically significant at the 6% level (using a one-tailed *t*-test).

The difference in prediction skill between the two methods of determining SCSSM onset may be in part related to the region used for the Gao et al. (2001) index; Wang et al. (2004) commented that: "... the northern SCS is open to the invasion of a cold front from the north. The westerly flow occurring before the onset is located north of the subtropical ridge and is not of tropical origin". They stated, therefore, that the northern part of the SCS should be excluded when defining the tropical monsoon burst over the SCS. He et al. (2017) also commented on the influence of northern cold air entering this region of the SCS contributing to ambiguous or intermittent onset. They highlighted the case of 2009, when the strong westerly flow established in mid April was interrupted by easterlies propagating from the northern SCS for several days in early May. Other examples of years where this occurred were given in He et al. (2017, Figs. 1 and 2), and included 2007, 2009 and 2011. Additionally, although He et al. (2017) did not identify 2004 as an intermittent onset year, the U_{850} averaged over the Gao et al. (2001) SCS box fluctuates between easterly and westerly during May, making the onset ambiguous when the Gao et al. (2001) index is used. He et al. (2017, Fig. 1) showed that this is related to the variability of the winds in the northern part of the SCS. In contrast, the U_{850} winds over the southern part of the SCS [as covered by the Wang et al. (2004) box] do not fluctuate to the same extent. Chan et al. (2000) showed that, in 1998, incursion of cold air into the northern SCS promoted the release of convective available potential energy, which helped to trigger the onset earlier than may have been expected given the ENSO conditions. Liu et al. (2002) further linked the cold-air incursion to a Rossby wave train triggered over the Bay of Bengal.

The additional influence of variability from the subtropics in the northern SCS, which, like ISO, is unpredictable on seasonal time scales, is likely to be a contributing factor in the reduced seasonal prediction skill for SCSSM onset using the Gao et al. (2001) criteria. In recognition of this, forecasters at CMA release their SCSSM onset forecasts using the Gao et al. (2001) criteria only on the extended range (11–30 days) timescale (D. Zhang, personal communication, 30 March 2018), on which models have been shown in previous work to possess skill in predicting intraseasonal variability (e.g., Lee et al., 2015; Lim et al., 2018).

3.3. *Drivers of SCSSM onset predictability using the Wang et al. (2004) index*

Several studies have shown that ENSO is one of the main drivers of large-scale interannual variability in the Asian monsoon region (e.g., Zhou and Chan, 2007; Luo et al., 2016). Westerly (easterly) equatorial wind anomalies associated with El Niño (La Niña) and a weaker (stronger) Walker circulation are typically associated with negative (positive) SST anomalies over the SCS and a delayed (advanced) seasonal transition (He et al., 2017). This relationship is not symmetrical, however: He et al. (2017) suggested that both ISOs and changes in west–east thermal contrasts across the Indian Ocean and western Pacific can influence the timing of onset in La Niña years. Hardiman et al. (2018) found a similar asymmetry in the relationship between seasonal mean Yangtze River rainfall and ENSO in observations and hindcasts.

We also show on Fig. 1 the observed March Niño3.4 SST anomaly time series from HadISST1.1 (yellow line). The correlation coefficient between the ensemble-mean SCSSM onset pentad time series derived using the Wang et al. (2004) index and the Niño3.4 SST time series is 0.9, indicating that the predictable component of the hindcast SCSSM onset is driven mainly by ENSO, which itself is highly predictable on this time scale in GloSea5 (Scaife et al., 2014; MacLachlan et al., 2015). The correlation between observed estimates of SCSSM onset and the observed March Niño3.4 SST is rather lower (0.41), indicating the influence of other drivers of SCSSM onset variability that may not be predictable, particularly the ISO (e.g. Shao et al., 2015; Wang et al., 2018), which is itself subject to interannual variations relating to large-scale modes, such as the Pacific–Japan teleconnection (Li et al., 2014). The skill of the ensemble (0.5) is therefore marginally higher than using predicted ENSO conditions alone to predict monsoon onset, though both are skillful.

Figure 3a provides additional insight by showing the correlation between the ensemble-mean SCSSM onset dates for the 23 years from the hindcast and observed global monthly mean SSTs in March over the same period. This illustrates that the predictable part of the SCSSM onset from the hindcast is strongly correlated with an ENSO-like pattern of Pacific SSTs, consistent with the findings of Zhu and Li (2017). There is also a strong positive correlation with SSTs in the equatorial Indian Ocean, again indicating that warmer SSTs are associated with later SCSSM onset dates. For the observed onset dates derived from ERA-Interim (Fig. 3b), the

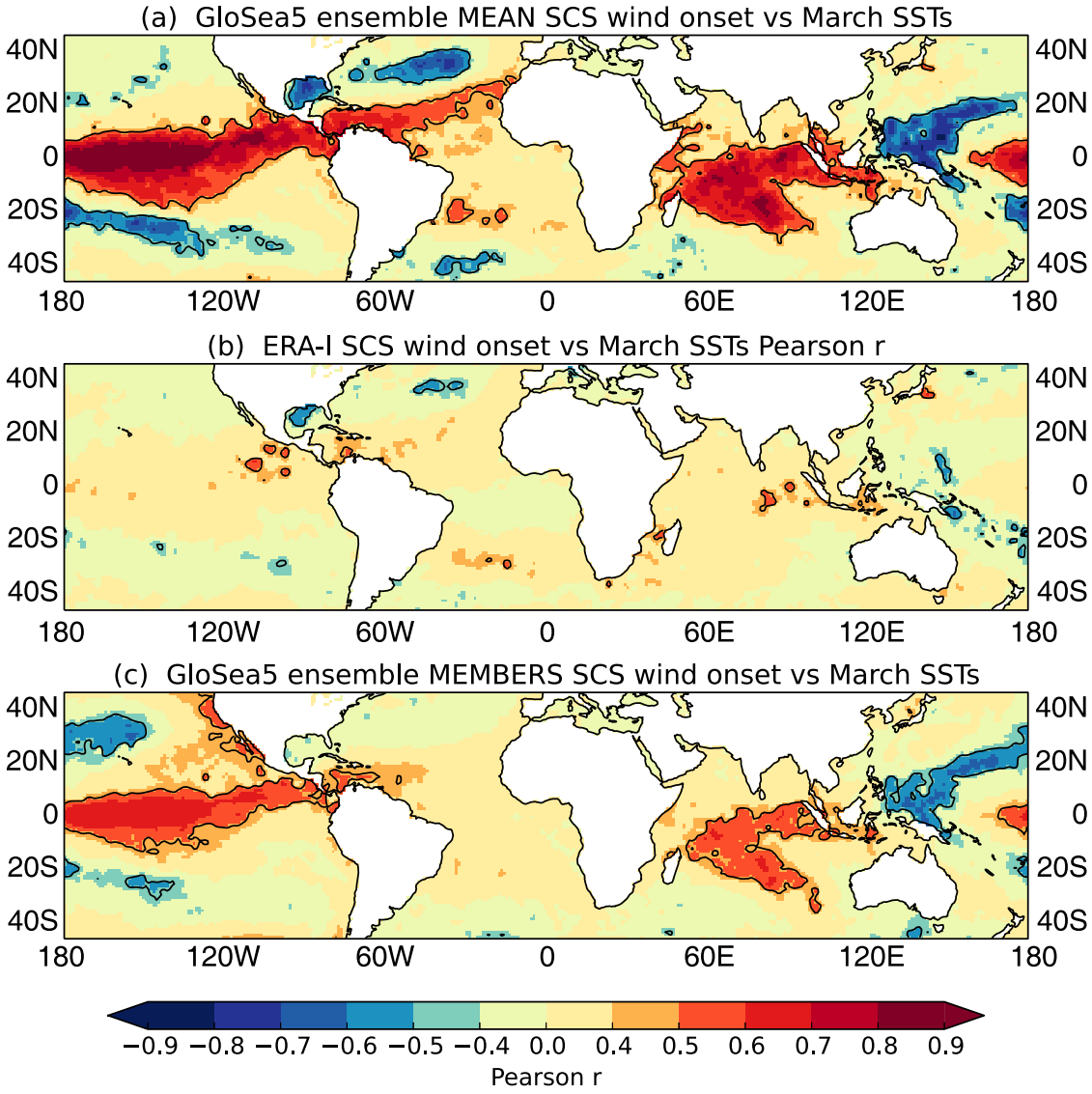

Fig. 3. Correlation coefficients between the SCSSM onset pentad derived using the Wang et al. (2004) index and observed March average SSTs from HadISST1.1 for the period 1993–2015, using: (a) ensemble-mean onset dates from the hindcast; (b) onset dates from ERA-Interim; (c) 10 000 pseudo-time-series of onset dates created by randomly selecting an individual ensemble member from each year (panel shows average over all correlations). Contours and darker shades indicate correlations significant at the 1% ($r = 0.48$) and 3% ($r = 0.40$) levels respectively, for a one-tailed t-test.

correlations with SST are far smaller, due to the presence of additional factors in the observations that are not predicted by the ensemble mean. The average correlations between the SSTs and 1000 pseudo-time-series of SCSSM onset created by randomly choosing an individual ensemble member hindcast for each year (Fig. 3c) are naturally smaller than with the ensemble-mean time series, but not as low as those in observations (Fig. 3b). This suggests that some of the subseasonal variations (e.g., ISOs) that affect SCSSM onset in reality may not be sufficiently well represented by the model to capture such influences, even at the relatively high horizontal resolution used by GloSea5 (N216; about 60 km at 50°N). This is consistent with the findings of Fang et al. (2016), who showed that while several aspects of the boreal summer ISO were improved in the Met Office Unified Model at this resolution, difficulty remained in realistic representation of the variance and propagation characteristics.

3.4. *Robustness of SCSSM wind onset predictability to ensemble size*

To assess the influence of ensemble size on the prediction skill using the Wang et al. (2004) index, we randomly sample small ensembles of between 1 and 51 members from the 52 members in our combined ensembles with start dates between 17 March and 9 April, and recalculate the correlation between the ensemble-mean time series and that from the observations for different numbers of ensemble members. Figure 4 indicates that, for this measure of monsoon

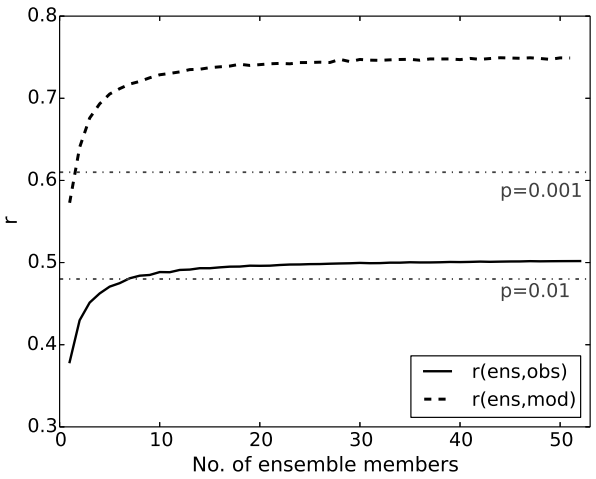

Fig. 4. Effect of ensemble size on the skill of SCSSM onset predictions using the Wang et al. (2004) index (solid line), denoted r (ens, obs), and the signal-to-noise ratio (correlation of ensemble-mean time series with a pseudo-time-series created by randomly selecting a single model ensemble member for each year; dashed line), denoted r (ens, mod). In both cases, for each choice of ensemble size, up to 10 000 ensemble-mean time series are generated by randomly selecting the chosen number of ensemble member onset dates (independently and without replacement) from the 52 onset dates diagnosed in each year in the combined ensemble and averaging over the chosen number of ensemble members. Dot-dashed lines indicate the values of r that are significant at the 1% and 0.1% levels for a one-tailed t-test.

onset, the prediction skill (black line) rises quickly with ensemble size, reaching a mean value of 0.5 for a 28-member ensemble (which is the size of the standard operational hindcast set), and is robust (correlation coefficients averaged over all ensemble-mean time series are statistically significant at the 1% level for a one-tailed test) for around 10 ensemble members or more. This is a reflection of the strong and predictable influence of ENSO on wider tropical rainfall (Kumar et al., 2013; Scaife et al., 2017) and, here, on the SCSSM onset dates in the hindcast: in most of the summers following strong El Niño/La Niña years (e.g., 1998, 1999, 2000, 2001, 2005, 2008, 2010), the spread among ensemble members is small and several members identify the same onset pentad (see Fig. 1), thereby constraining the values selected by random sampling of the ensemble for those years.

Several authors (e.g., Eade et al., 2014; Scaife et al., 2014; Dunstone et al., 2016) have demonstrated that the model's North Atlantic Oscillation is less predictable than that observed, so that a large number of ensemble members is required for good prediction skill. This was confirmed by repeatedly randomly selecting a single member to be the truth and using the ensemble mean of the remaining members to predict that member. In contrast, the dashed line in Fig. 4 indicates that the model's SCSSM onset dates are more predictable than those from reanalyses, i.e., that the model is over-confident in its predictions, as is often found for tropical rainfall (Weisheimer and Palmer, 2014). This again illustrates the dominant role of ENSO in providing the predictability in the model, while the observed onset dates are also influenced by intraseasonal variations that are unpredictable on the seasonal time scale.

4. Conclusions

SCSSM onset, as determined by the Wang et al. (2004) U_{850} wind index, is skillfully predicted in GloSea5 at up to a three-month lead time, particularly during active ENSO years. Since the SCSSM onset signifies the start of the broadscale EASM, its skillful prediction is important for forecasters as an indicator of the possible characteristics of the season to come. This complements the skill previously demonstrated for predicting seasonal-mean precipitation in the Yangtze River region (Li et al., 2016). The prediction skill for SCSSM onset using this index is robust even with only around 10 ensemble members, consistent with skill in prediction of rainfall in the deep tropics (e.g. Scaife et al., 2017). The skill is largely related to ENSO SSTs, which have been shown to be highly predictable in the GloSea5 seasonal forecasting system.

In contrast, the Gao et al. (2001) SCSSM onset index, which includes an increase of θ_e in the SCS region as a measure of thermodynamic onset alongside the change to westerly winds, shows little predictability on seasonal time scales. We speculate that this is partly due to the region used by Gao et al. (2001), as this includes the northern SCS, which can be influenced by incursions of cold air from the north. This additional influence is, like the ISO, inherently unpredictable on the seasonal time scale, and thus its inclusion through the northward extension of the box used for the Gao et al. (2001) index compared with that of Wang et al. (2004) is, in our view, a contributing factor in the reduced seasonal prediction skill. However, we propose that a seasonal forecast of the broadscale transition using the Wang et al. (2004) index would provide some useful early information for forecasters, and their guidance could later be refined, using other measures such as the Gao et al. (2001) index, with medium-range forecasts that may capture the influence of intraseasonal variations at shorter lead times.

He and Zhu (2015) investigated the correlations between the SCSSM onset [as determined by the Wang et al. (2004) criteria] and the subsequent EASM rainfall from May to September in observations/reanalyses. They suggested that, in contrast with the traditional view that a later onset date would be associated with a lower-than-normal total seasonal rainfall amount, the region from the lower Yangtze River to Korea and southern Japan shows a positive correlation between the SCSSM onset date and the seasonal mean rainfall, i.e., early SCSSM onset tends to be followed by lower-than-normal seasonal-mean rainfall further north. He and Zhu (2015) associate this relationship with a persistent western North Pacific anticyclonic/cyclonic anomaly accompanied by decaying El Niño/La Niña conditions in boreal spring to sum-

mer (Wu, 2010; Stuecker et al., 2013; Hardiman et al., 2018). This suggests that skillful predictions of SCSSM onset could provide an indication of the seasonal-mean rainfall in parts of the EASM region.

To the best of our knowledge, this is the first time that skill in predicting the broadscale transition associated with the SCSSM onset on seasonal time scales in an operational dynamical forecasting system has been demonstrated. We encourage other centers to investigate this in their operational forecasting systems. While it is recognized that the onset and progression of the SCSSM and EASM systems is complex and may be influenced by other factors, such as synoptic events, intraseasonal variability and regional air–sea interactions with little or no predictability on the seasonal time scale, the ability to provide skillful predictions of whether the broadscale seasonal transition is likely to be early, late or normal provides useful, early information for local forecasters, particularly when combined with other predictions, such as the Yangtze River basin rainfall, which have also been shown to be skillful (Li et al., 2016) and are now provided in real time to the CMA (Bett et al., 2018).

Acknowledgements. This work and its contributors (GM, AC, RC, ND and AS) were supported by the UK–China Research & Innovation Partnership Fund through the Met Office Climate Science for Service Partnership (CSSP) China as part of the Newton Fund. DZ was supported by the National Natural Science Foundation of China (Grant No. 41605078).

REFERENCES

Bett, P. E., and Coauthors, 2018: Seasonal forecasts of the summer 2016 Yangtze River basin rainfall. *Adv. Atm. Sci.*, **35**, 918–926, https://doi.org/10.1007/s00376-018-7210-y.

Bolton, D., 1980: The computation of equivalent potential temperature. *Mon. Wea. Rev.*, **108**, 1046–1053, https://doi.org/10.1175/1520-0493(1980)108<1046:TCOEPT>2.0.CO;2.

Chan, J. C. L., Y. G. Wang, and J. J. Xu, 2000: Dynamic and thermodynamic characteristics associated with the onset of the 1998 South China Sea summer monsoon. *J. Meteor. Soc. Japan*, **78**, 367–380, https://doi.org/10.2151/jmsj1965.78.4_367.

Dee, D. P., and Coauthors, 2011: The ERA-Interim reanalysis: Configuration and performance of the data assimilation system. *Quart. J. Roy. Meteor. Soc.*, **137**, 553–597, https://doi.org/10.1002/qj.828.

Ding, Y. H., and J. C. L. Chan, 2005: The East Asian summer monsoon: An overview. *Meteor. Atmos. Phys.*, **89**, 117–142, https://doi.org/10.1007/s00703-005-0125-z.

Ding, Y. H., and C. He, 2006: The summer monsoon onset over the tropical eastern Indian Ocean: The earliest onset process of the Asian summer monsoon. *Adv. Atmos. Sci*, **23**, 940–950, https://doi.org/10.1007/s00376-006-0940-2.

Dunstone, N., D. Smith, A. Scaife, L. Hermanson, R. Eade, N. Robinson, M. Andrews, and J. Knight, 2016: Skilful predictions of the winter North Atlantic Oscillation one year ahead. *Nature Geoscience*, **9**, 809–814, https://doi.org/10.1038/ngeo2824.

Eade, R., D. Smith, A. Scaife, E. Wallace, N. Dunstone, L. Hermanson, and N. Robinson, 2014: Do seasonal-to-decadal climate predictions underestimate the predictability of the real world? *Geophys. Res. Lett.*, **41**, 5620–5628, https://doi.org/10.1002/2014GL061146.

Fang, Y. J., and Coauthors, 2016: High-resolution simulation of the boreal summer intraseasonal oscillation in Met Office Unified model. *Quart. J. Roy. Meteor. Soc.*, **143**, 362–373, https://doi.org/10.1002/qj.2927.

Gao, H., Y. K. Tan, and J. J. Liu, 2001: Definition of 40-year onset date of South China Sea Summer Monsoon. *Journal of Nanjing Institute of Meteorology*, **24**, 379–383, https://doi.org/10.3969/j.issn.1674-7097.2001.03.012. (in Chinese with English abstract)

Hardiman, S. C., and Coauthors, 2018: The asymmetric response of Yangtze river basin summer rainfall to El Niño/La Niña. *Environmental Research Letters*, **13**(2), 024015, https://doi.org/10.1088/1748-9326/aaa172.

He, B., Y. Zhang, T. Li, and W.-T. Hu, 2017: Interannual variability in the onset of the South China Sea summer monsoon from 1997 to 2014. *Atmospheric and Oceanic Science LettersLetterLetter*, **10**, 73–81, https://doi.org/10.1080/16742834.2017.1237853.

He, J. H., and Z. W. Zhu, 2015: The relation of South China Sea monsoon onset with the subsequent rainfall over the subtropical East Asia. *International Journal of Climatology*, **35**, 4547–4556, https://doi.org/10.1002/joc.4305.

He, Z. Q., and R. G. Wu, 2013: Seasonality of interannual atmosphere–ocean interaction in the South China Sea. *Journal of Oceanography*, **69**, 699–712, https://doi.org/10.1007/s10872-013-0201-9.

Hu, W. T., R. G. Wu, and Y. Liu, 2014: Relation of the South China Sea precipitation variability to tropical Indo-Pacific SST anomalies during spring-to-summer transition. *J. Climate*, **27**, 5451–5467, https://doi.org/10.1175/JCLI-D-14-00089.1.

Kalnay, E., and Coauthors, 1996: The NCEP/NCAR 40-year reanalysis project. *Bull. Amer. Meteor. Soc.*, **77**, 437–472, https://doi.org/10.1175/1520-0477(1996)077<0437:TNYRP>2.0.CO;2.

Kanamitsu, M., W. Ebisuzaki, J. Woollen, S. K. Yang, J. J. Hnilo, M. Fiorino, and G. L. Potter, 2002: NCEP–DOE AMIP-II reanalysis (R-2). *Bull. Amer. Meteor. Soc.*, **83**, 1631–1643, https://doi.org/10.1175/BAMS-83-11-1631.

Kumar, A., M. Y. Chen, and W. Q. Wang, 2013: Understanding prediction skill of seasonal mean precipitation over the Tropics. *J. Climate*, **26**, 5674–5681, https://doi.org/10.1175/JCLI-D-12-00731.1.

Lau, K. M., and S. Yang, 1997: Climatology and interannual variability of the Southeast Asian summer monsoon. *Adv. Atmos. Sci.*, **14**, 141–162, https://doi.org/10.1007/s00376-997-0016-y.

Lee, S. S., B. Wang, D. E. Waliser, J. M. Neena, and J.-Y. Lee, 2015: Predictability and prediction skill of the boreal summer intraseasonal oscillation in the Intraseasonal Variability Hindcast Experiment. *Climate Dyn.*, **45**, 2123–2135, https://doi.org/10.1007/s00382-014-2461-5.

Li, C. F., and Coauthors, 2016: Skillful seasonal prediction of Yangtze river valley summer rainfall. *Environmental Research Letters*, **11**(9), 094002, https://doi.org/10.1088/1748-9326/11/9/094002.

Li, H., S. P. He, K. Fan, and H. J. Wang, 2018: Relationship between the onset date of the Meiyu and the South Asian anticyclone in April and the related mechanisms. *Climate Dyn.*,

https://doi.org/10.1007/s00382-018-4131-5.

Li, K. P., W. D. Yu, T. Li, V. S. N. Murty, S. Khokiattiwong, T. R. Adi, and S. Budi, 2013: Structures and mechanisms of the first-branch northward-propagating intraseasonal oscillation over the tropical Indian Ocean. *Climate Dyn.*, **40**, 1707–1720, https://doi.org/10.1007/s00382-012-1492-z.

Li, R. C. Y., W. Zhou, and T. Li, 2014: Influences of the Pacific–Japan teleconnection pattern on synoptic-scale variability in the Western North Pacific. *J. Climate*, **27**, 140–154, https://doi.org/10.1175/JCLI-D-13-00183.1.

Lim, Y., S. W. Son, and D. Kim, 2018: MJO prediction skill of the subseasonal-to-seasonal prediction models. *J. Climate*, **31**, 4075–4094, https://doi.org/10.1175/JCLI-D-17-0545.1.

Liu, Y. M., J. C. L. Chan, J. Y. Mao, and G. X. Wu, 2002: The role of Bay of Bengal convection in the onset of the 1998 South China Sea summer monsoon. *Mon. Wea. Rev.*, **130**, 2731–2744, https://doi.org/10.1175/1520-0493(2002)130<2731:TROBOB>2.0.CO;2.

Luo, M., and L. J. Lin, 2017: Objective determination of the onset and withdrawal of the South China Sea summer monsoon. *Atmospheric Science Letters*, **18**, 276–282, https://doi.org/10.1002/asl.753.

Luo, M., Y. Leung, H. F. Graf, M. Herzog, and W. Zhang, 2016: Interannual variability of the onset of the South China Sea summer monsoon. *International Journal of Climatology*, **36**, 550–562, https://doi.org/10.1002/joc.4364.

Luo, Y. L., H. Wang, R. H. Zhang, W. M. Qian, and Z. Z. Luo, 2013: Comparison of rainfall characteristics and convective properties of monsoon precipitation systems over south China and the Yangtze and Huai River basin. *J. Climate*, **26**, 110–132, https://doi.org/10.1175/JCLI-D-12-00100.1.

MacLachlan, C., and Coauthors, 2015: Global Seasonal forecast system version 5 (GloSea5): A high-resolution seasonal forecast system. *Quart. J. Roy. Meteor. Soc.*, **141**, 1072–1084, https://doi.org/10.1002/qj.2396.

Rayner, N. A., D. E. Parker, E. B. Horton, C. K. Folland, L. V. Alexander, D. P. Rowell, E. C. Kent, and A. Kaplan, 2003: Global analyses of sea surface temperature, sea ice, and night marine air temperature since the late nineteenth century. *J. Geophys. Res.*, **108**, 4407, https://doi.org/10.1029/2002JD002670.

Sampe, T., and S. P. Xie, 2010: Large-scale dynamics of the Meiyu–Baiu rainband: Environmental forcing by the westerly jet. *J. Climate*, **23**, 113–134, https://doi.org/10.1175/2009JCLI3128.1.

Scaife, A. A., and Coauthors, 2014: Skillful long-range prediction of European and North American winters. *Geophys. Res. Lett.*, **41**, 2514–2519, https://doi.org/10.1002/2014GL059637.

Scaife, A. A., and Coauthors, 2017: Tropical rainfall, Rossby waves and regional winter climate predictions. *Quart. J. Roy. Meteor. Soc.*, **143**, 1–11, https://doi.org/10.1002/qj.2910.

Shao, X., P. Huang, and R.-H. Huang, 2015: Role of the phase transition of intraseasonal oscillation on the South China Sea summer monsoon onset. *Climate Dyn.*, **45**, 125–137, https://doi.org/10.1007/s00382-014-2264-8.

Stuecker, M. F., A. Timmermann, F. F. Jin, S. McGregor, and H. L. Ren, 2013: A Combination mode of the annual cycle and the El Niño/Southern Oscillation. *Nature Geoscience*, **6**, 540–544, https://doi.org/10.1038/ngeo1826.

Tao, S.-Y., and L.-X. Chen, 1987: Review of recent research on the East Asian summer monsoon in China. *Monsoon Meteorology*, C.-P. Chang and T. N. Krishnamurti, Eds., Oxford University Press, 60–92.

Wang, B., F. Huang, Z. W. Wu, J. Yang, X. H. Fu, and K. Kikuchi, 2009: Multi-scale climate variability of the South China Sea monsoon: A review. *Dyn. Atmos. Oceans*, **47**, 15–37, https://doi.org/10.1016/j.dynatmoce.2008.09.004.

Wang, B., LinHo, Y. S. Zhang, and M. M. Lu, 2004: Definition of South China Sea monsoon onset and commencement of the East Asia summer monsoon. *J. Climate*, **17**, 699–710, https://doi.org/10.1175/2932.1.

Wang, H., F. Liu, B. Wang, and T. Li, 2018: Effects of intraseasonal oscillation on South China Sea summer monsoon onset. *Climate Dyn.*, **51**, 2543–2558, https://doi.org/10.1007/s00382-017-4027-9.

Weisheimer, A., and T. N. Palmer, 2014: On the reliability of seasonal climate forecasts. *Journal of the Royal Society Interface*, **11**, 20131162, https://doi.org/10.1098/rsif.2013.1162.

Williams, K. D., and Coauthors, 2015: The Met Office Global Coupled model 2.0 (GC2) configuration, *Geoscientific Model Development*, **8**, 1509–1524, https://doi.org/10.5194/gmd-8-1509-2015.

Wu, B., T. Li, and T. Zhou, 2010: Relative contributions of the Indian Ocean and local SST anomalies to the maintenance of the Western North Pacific anomalous anticyclone during the El Niño decaying summer. *J. Climate*, **23**, 2974–2986, https://doi.org/10.1175/2010JCLI3300.1.

Wu, G. X., Y. M. Liu, B. He, Q. Bao, A. M. Duan, and F. F. Jin, 2012: Thermal controls on the Asian summer monsoon. *Nature Scientific Reports*, **2**, 404, https://doi.org/10.1038/srep00404.

Wu, R. G., 2010: Subseasonal variability during the South China Sea summer monsoon onset. *Climate Dyn.*, **34**, 629–642, https:// doi.org/10.1007/s00382-009-0679-4.

Xie, S. P., Y. Kosaka, Y. Du, K. M. Hu, J. S. Chowdary, and G. Huang, 2016: Indo-western Pacific ocean capacitor and coherent climate anomalies in post-ENSO summer: A review. *Adv. Atmos. Sci.*, **33**, 411–432, https://doi.org/10.1007/s00376-015-5192-6.

Zhou, W., and J. C. L. Chan, 2007: ENSO and the South China Sea summer monsoon onset. *International Journal of Climatology*, **27**, 157–167, https://doi.org/10.1002/joc.1380.

Zhu, Z. W., and J. H. He, 2013: The vortex over Bay of Bengal and its relationship with the outbreak of South China Sea summer monsoon. *Journal of Tropical Meteorology*, **29**, 915–923. (in Chinese with English abstract)

Zhu, Z. W., and T. Li, 2017: Empirical prediction of the onset dates of South China Sea summer monsoon. *Climate Dyn.*, **48**, 1633–1645, https://doi.org/10.1007/s00382-016-3164-x.